

Green zero-valent iron nanoparticles for the degradation of amoxicillin

S. Machado¹ · J. G. Pacheco¹ · H. P. A. Nouws¹ · J. T. Albergaria¹

C. Delerue-Matos¹

Abstract In the last years, it has been proven that zero-valent iron nanoparticles, including those produced using green methods, are efficient remediation agents for a wide range of target contaminants. However, apart from the known advantages of these green nanomaterials, the knowledge of how they act on distinct contaminants is not yet fully understood and requires further investigation. The objectives of this work were to study the degradation of a common antibiotic, amoxicillin, in water and in a sandy soil using green zero-valent iron nanoparticles (gnZVIs) as reductants and as catalysts for the Fenton reaction. It represents the first study of the use of gnZVI, as alternative for the zero-valent iron nanoparticles produced with sodium borohydride, for the degradation of amoxicillin. The results of the performed tests indicate that gnZVIs have the potential to be used in remediation processes. In both chemical tests, the gnZVI was able to degrade up to 100% of amoxicillin in aqueous solutions, using an amoxicillin/gnZVI molar ratio of 1:15 when applied as a reductant, and an amoxicillin/H₂O₂/gnZVI molar ratio of 1:13:1 when applied as a catalyst for the Fenton reaction. The soil tests showed that the required molar ratios for near complete degradation were higher in the reduction test (1:150) than in the gnZVI-catalyzed Fenton reaction (1:1290:73). This is possibly due to parallel reactions with the soil matrix and/or limitations of the reagents to reach the entire soil sample. The degradation efficiencies obtained in these tests

were 55 and 97% for the reduction and catalyzed Fenton processes, respectively.

Keywords Green zero-valent iron nanoparticles · Amoxicillin · Soil · Water · Fenton · Catalyst · Environmental remediation

Introduction

Nanotechnology is one of the scientific domains that has presented the most significant developments in the last decades. Among the different branches of nanotechnology, environmental nanoremediation is highlighted in this work; it involves the application of reactive nanoscale materials for the transformation and detoxification of contaminants in distinct environmental compartments (Karn et al. 2009; Saravanan et al. 2011). The small size of the nanoparticles as well as their high reactivity makes them excellent options to remediate water and soils because they can infiltrate into very small pores of the soil and can also persist suspended in the groundwater, allowing the nanoparticles to move farther away from the injection point. Nevertheless, some studies showed that in real situations the nanomaterials are not found very far from the injection points (Tratnyek and Johnson 2006).

There are several materials that are used to produce nanoparticles for environmental remediation such as metal oxides, (noble) metals and bimetallic combinations, and carbon-based materials (Gottschalk et al. 2013; Gupta et al. 2013; Matlochova et al. 2013; Saravanan et al. 2013).

It has already been recognized that zero-valent iron is the most common nanoparticles used for soil remediation, and it is effective in the removal of a wide range of both organic and inorganic contaminants from water and soil

Editorial responsibility: V.K. Gupta.

✉ J. T. Albergaria
jtva@isep.ipp.pt

¹ Requite/IAQV, Instituto Superior de Engenharia do Porto, Instituto Politécnico do Porto, Rua Dr. António Bernardino de Almeida, 431, 4200-072 Porto, Portugal

(Blowes et al. 2000; Cundy et al. 2008; O'Hannesin and Gillham 1998; Saleh and Gupta 2012; Wang et al. 2012). In the last 15 years, the use and research on the remediation technologies involving nZVI has increased exponentially, with dozens of pilot and full-scale operations taking place worldwide and a massive number of published scientific documents (Yan et al. 2013), demonstrating the importance of this material for environmental remediation. This is the reason that iron nanoparticles were chosen for this work.

nZVI can be produced by top-down and bottom-up approaches, in the former procedure, particles with larger dimensions (micro and granular particles) are transformed into nanostructures through mechanical and/or chemical processes (Li et al. 2006), and in the latter procedure, atom-by-atom or molecule-by-molecule structures are "grown" through chemical synthesis, positional or self-assembling (Wang and Zhang 1997). The top-down methods, which include the decomposition of iron pentacarbonyl ($\text{Fe}(\text{CO})_5$) in organic solvents (Karlsson et al. 2005) and vacuum sputtering (Kuhn et al. 2002), are generally expensive and require specific and costly equipment (Li et al. 2006). The bottom-up methods can be divided in two major groups: the traditional and the green methods. The traditional method involves the reaction of iron(II) or iron(III) salts with sodium borohydride and is a simple method in which only common laboratory reagents and equipment are required. However, there are several safety issues to be considered when employing this method such as the toxicity of sodium borohydride and the production of flammable hydrogen gas. Furthermore, the nanoparticles produced by this process tend to agglomerate rapidly, reducing their reactivity and degradation efficiency (Li et al. 2006). The green production method is more recent and uses extracts from natural products such as tree leaves (Chrysochoou et al. 2012; Hoag et al. 2009). These extracts have high antioxidant capacities, and its constituents react with iron(III) in solution to form the gnZVIs that can degrade different types of contaminants such as dyes (Hoag et al. 2009), metals (Chrysochoou et al. 2012), and pharmaceutical products (Machado et al. 2013b). The advantages of this synthesis method are: (1) the use of a non-toxic reducing agent; (2) the capping of the gnZVIs by the polyphenol extract matrix, which prolongs their reactivity; (3) the valorization of natural products that, in most cases, are considered wastes; and (4) the enhancement of complementary biodegradation with the extracts as nutrient source. Although these advantages turn the use of this nanomaterial extremely attractive, its applications are not yet fully studied. The gnZVIs, when compared to traditional nZVI,

have a natural capping allowing them to persist reactive more time, less tendency to agglomerate, are amorphous in nature and could be found and produced in smaller sizes (Machado et al. 2013a; Stefaniuk et al. 2016).

In recent years, nZVI has also been used as a catalyst for the Fenton reaction and was applied to the degradation of contaminants (Kuang et al. 2013; Wang et al. 2010; Xu and Wang 2013). However, studies involving the use of gnZVI for this purpose are scarce and also require further investigation. Following this and in order to gather more information, the application of gnZVIs to the degradation of an antibiotic (amoxicillin (AMX)) through reduction and gnZVI-catalyzed Fenton processes is studied in this work. This work was developed in 2015–2016 in Porto, Portugal.

Materials and methods

Reagents

All the reagents used throughout the work were of analytical grade or equivalent quality. Amoxicillin (AMX) and ammonium iron(II) sulfate heptahydrate were obtained from Sigma-Aldrich, hydrogen peroxide (30% (w/v)) and sodium hydroxide were purchased from Panreac, hydrochloric acid ($\geq 36.5\%$) was obtained from Carlo Erba, and HPLC-grade acetonitrile, formic acid, sodium hydroxide, and iron(III) chloride hexahydrate were obtained from Merck.

The type I deionized water (resistivity = 18.2 M Ω cm) used in all the studies was obtained from a Simplicity 185 water purification system (Millipore).

Analysis of amoxicillin

AMX was analyzed with a Waters 2795 Alliance HT liquid chromatographic (LC) system equipped with a Kinetex 2.6 μm C₁₈ 100 Å (100 \times 4.60 mm) column, a column oven (set at 35 °C), an automatic injection valve (V_{inj} = 20 μL), and a Waters 2996 photodiode array detector (PAD, λ_{det} = 230 nm). The mobile phase flow was set at 0.5 mL min⁻¹ and was composed of mixture of a 0.1% (v/v) aqueous formic acid solution (A) and a 0.1% (v/v) formic acid solution in acetonitrile (B). The following gradient program was used: A/B (% (v/v)): 94/6: 0–3 min, 20/80: 6–8 min; 94/6: 10–20 min.

AMX was quantified in the samples by the external standard calibration method (calibration curves between 0.1 and 10.0 mg L⁻¹ were constructed ($r > 0.9988$)).

Synthesis and characterization of gnZVI

The leaf extracts were produced in a glass flask with 3.7 g milled oak leaves and 100 mL of water, the mixture was then heated at 80 °C in a shaker bath for 20 min, and the final solution was filtered to remove the used leaves (Machado et al. 2013a). The production of gnZVI was achieved by mixing a 0.100-mol L⁻¹ iron(III) chloride solution with the leaf extract solution, in excess, to guarantee the total conversion of the iron(III) to zero-valent iron, allowing to consider that the amount of gnZVI produced corresponds to the amount of iron(III) added. For oak leaves extract, the most appropriate mixing ratio is 15 µL Fe(III)/mL extract.

For the Transmission Electronic Microscopy (TEM) analysis, the oak gnZVIs were mounted on 300-mesh nickel grids and examined using a JEOL JEM 1400 Transmission Electronic Microscope (120 kV). Magnifications from 120,000 to 500,000× were used to determine the size of the nZVIs (measured directly on the TEM image using the software of the equipment). Energy-dispersive X-ray spectroscopy (EDS) analyses were also conducted to determine the composition of the gnZVIs.

The X-ray diffraction (XRD) analysis was performed on a solid nZVI sample in the 2θ angle range (0°–90°) with a step size of 0.04°.

Reduction of AMX in aqueous solution by gnZVI

The reduction tests were performed in Erlenmeyer flasks containing 25 mL of a 10-mg L⁻¹ AMX solution. Different amounts of gnZVI were added to the AMX solution, by mixing different volumes of oak leaf extract and iron(III) solution (corresponding to distinct AMX/gnZVI molar ratios) promoting the reaction between the nanomaterial and the AMX. The production of the gnZVI occurring in the bulk of the contaminated solution will reduce the parallel reactions between the gnZVIs and other surrounding compounds, e.g., oxidation by the atmospheric oxygen enhancing the process efficiency. Samples from the reaction mixture were collected along the process and analyzed by LC. Similar tests were performed with AMX and oak leaf extracts (no gnZVI production) to evaluate the individual effect of the extract on the degradation of AMX. Control tests were also performed in order to evaluate the natural degradation of AMX.

Degradation of AMX through a gnZVI-catalyzed Fenton reaction in aqueous solution

Several tests with gnZVI, produced with oak leaf extracts, as catalyst for the Fenton reaction were carried out in

Erlenmeyer flasks with 25 mL of 10 mg L⁻¹ AMX solutions with different amounts of hydrogen peroxide and gnZVI. Traditional Fenton reaction experiments with hydrogen peroxide and iron (II) (using similar reagents molar ratios) were also executed in order to compare results. All this set of tests were performed at different pHs (3 and 7), adjusted with hydrochloric acid and sodium hydroxide solutions.

Enhanced biodegradation of AMX with the natural extract

The tree leaves, which have natural products, carry microorganisms that could have an important role in biological processes during the chemical tests. To evaluate the weight of this processes, tests were performed to evaluate the ability of the oak leaf extract to enhance the (bio)degradation of AMX. These tests were performed in Erlenmeyer flasks with 25 mL of 10-mg L⁻¹ AMX and amounts of oak extract similar to those indicated in sections “[Reduction of AMX in aqueous solution by gnZVI](#)” and “[Degradation of AMX through a gnZVI-catalyzed Fenton reaction in aqueous solution.](#)”

Remediation of a sandy soil by gnZVI

The sandy soil was purchased from Mibal–Minas de Barqueiros, S.A. (Esposende, Portugal) and was composed of particles with diameters between 0.5 and 1 mm. The soil did not contain detectable organic matter and had a pH of 6.27 and an apparent density of 1.38 g mL⁻¹.

The sandy soils were previously prepared to induce the desired AMX contamination. This preparation involved three steps: (1) drying of the soil at 105 °C (for 24 h), (2) addition of a standard aqueous AMX solution (100 mg L⁻¹) to induce the contamination (5 mg kg⁻¹), and (3) homogenization of the soil. At the same time, a non-contaminated soil was prepared following the same procedure, replacing the AMX solution with deionized water.

Based on previous experiments elaborated within the aim of this work, the complete extraction of AMX from the soil was assured by the addition of 30 mL of a 0.025-mol L⁻¹ NaOH solution to 50 g of contaminated soil, followed by stirring for 10 min. An aliquot of the resulting suspension was then centrifuged at 14,000 rpm for 5 min, and the supernatant was analyzed by LC.

The soil tests were performed in glass tubes (i.d.: 2.5 cm; h: 14.5 cm) in which 50 g of contaminated soil was placed. For the chemical reduction tests, the gnZVIs were produced in the soil matrix by injecting the oak leaf extract followed by the injection of a 0.100-mol L⁻¹ iron(III) solution. In each hour, the AMX was extracted from the soil sample and analyzed by LC. The experiments with

the catalyzed Fenton reaction were performed in the same way described above for the reduction tests, injecting a hydrogen peroxide solution immediately after the iron(III) solution. A traditional Fenton process was performed in the same way to compare the results.

Results and discussion

Synthesis and characterization of gnZVI

The procedure to synthesize the gnZVI presents several advantages when compared with the traditional sodium borohydride method, namely the simplicity of the procedure, the utilization of simple materials and equipment, the low cost, and the avoidance to use toxic reagents.

This synthesis method uses natural products such as tree leaves (Machado et al. 2013a) or wastes from food industries (Machado et al. 2014) to produce a natural extract with high antioxidant power capable to transform the iron(III) in amorphous (concluded after the XRD analysis) zero-valent nanoparticles, substituting the sodium borohydride. The fact that the gnZVIs are produced when the iron(III) solution contacts with the natural extract allows to perform the synthesis exactly where the contaminant really is and without loss of reactivity due to parallel reaction with the surrounding oxygen during transport in the contaminated media.

The characterization of several gnZVI produced with distinct tree leaves (size, shape, reactivity, and agglomeration tendency) is presented in Machado et al. (2015)). The gnZVIs produced with oak leaves presented sizes between 20 and 100 nm and have irregular shapes probably due to distinct reaction times and the complexity of the extract composition (Wang et al. 2014). Depending on the nature of the extract, distinct types of agglomeration can occur, cloud-type, net-type, and large-structured, being the former the type observed on the oak leaves gnZVI. The EDS analysis showed that the oak leaves nanoparticles were constituted by iron but also presented a high carbon, oxygen (from the polyphenols of the extract that act as capping agent), and chlorine (from the iron chloride solution used to produce the nZVI) (Machado et al. 2015).

Remediation of aqueous solutions

Reduction of AMX in aqueous solution by gnZVI

In Fig. 1, the degradation profiles of AMX obtained in the reduction tests with different AMX/gnZVI molar ratios

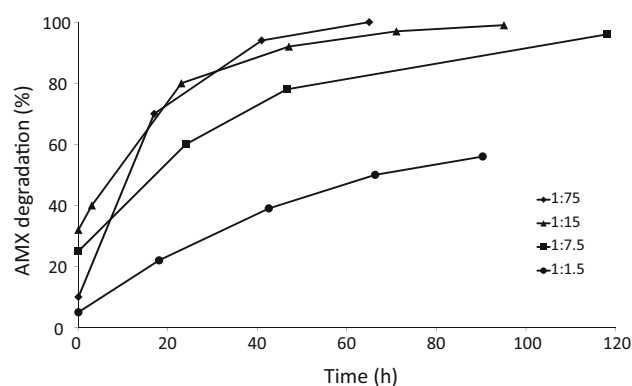


Fig. 1 Degradation of AMX in aqueous solutions by gnZVI

(from 1:1.5 to 1:75) are presented. It can be observed that higher amounts of gnZVI led to the increase in the degradation of AMX: from 50% with the 1:1.5 ratio to 100% with the 1:75 ratio, after a 60-min reaction time. These tests were performed in the presence of atmospheric oxygen that promotes the formation of a thin iron oxide layer on the nanoparticles, thus hindering the reaction between the gnZVI and AMX (Ghauch et al. 2009). In all studied ratios, a first fast degradation rate was observed, after which the reaction tended to slow down because of the accumulation of several final and intermediate products on/near the gnZVI particles. This behavior is in agreement with other studies that described the AMX removal as a combination of physical and chemical mechanisms when in contact with nZVI: A fast reduction step followed by adsorption of AMX onto the iron corrosion products and finally capture of AMX by the iron hydroxides (Zha et al. 2014). It is known the important role that adsorption has on degradation processes with several nanoparticles and with several contaminants (Saleh et al. 2015; Saleh and Gupta 2011; Waalewijn-Kool et al. 2013).

A degradation mechanism was proposed by Ghauch et al. (2009) that indicated that AMX is rapidly transformed to AMX penicilloic acid (through b-lactam ring opening) and then probably to undetectable AMX penilloic acid as end product due to decarboxylation reaction occurring with the free carboxyl group (Fig. 2). This proposal is in agreement with the results presented in Nägele and Moritz (2005).

An AMX/gnZVI molar ratio of 1:15 was considered to be the most appropriate because it provided the complete degradation of AMX present in the solution in less than 2 h (95 min). It is therefore unnecessary to use higher ratios just to reach a slightly faster total degradation. This shows that the use of gnZVI is an efficient, fast, easy, and low cost

Fig. 2 Degradation mechanism of AMX

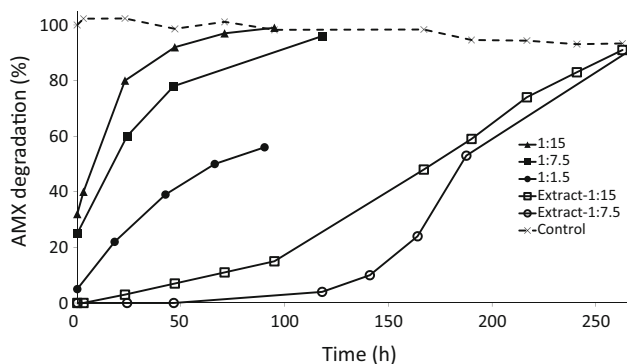
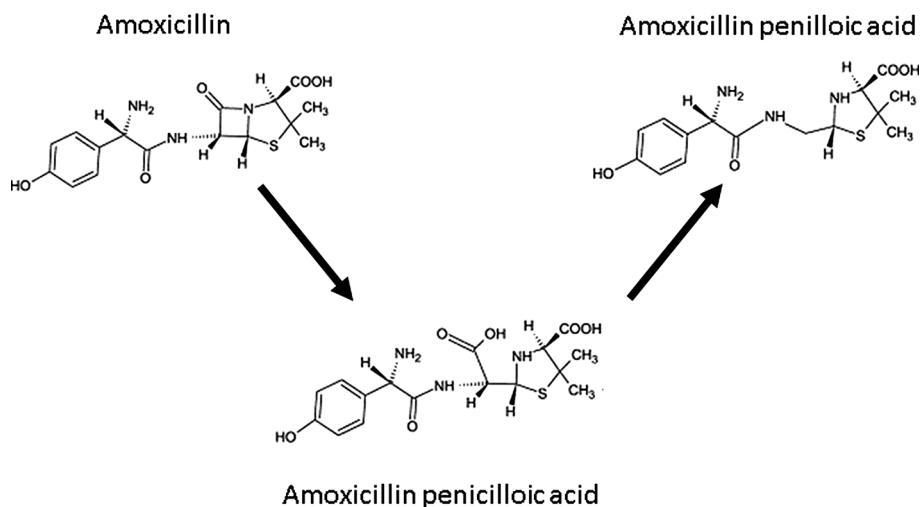


Fig. 3 Degradation of AMX in aqueous solutions by gnZVI and by natural extract

alternative for the degradation of AMX in aqueous systems.

In Fig. 3, the degradation profiles of AMX for different AMX/gnZVI molar ratios as well as the results obtained in the tests only with extract (same amount that was used in the gnZVI tests) (only for the 1:15 and 1:7.5 ratios) are presented. The tests with AMX and the extract aimed to evaluate their capacity to enhance biodegradation. As shown in Fig. 3, the AMX started to be degraded contin-

uously and intensely after 100–120 h, while the control remain stable, showing the existence of biological degradation that represents a valuable advantage of gnZVI because if the chemical action of the gnZVI does not achieve the defined remediation goals, the extract can continue to aid, as a nutrient or microbial source, in the biological degradation of AMX and finalize the remediation process. This shows that the degradation of AMX by the gnZVI consists on the combination of physical, chemical but also biological interactions between the AMX the gnZVI but also with the natural extract. At a first stage occurs physical (namely sorption mechanisms) and chemical (redox reactions) processes followed by biological degradation processes (Machado et al. 2013b; Zha et al. 2014).

In Table 1, the values of the observed first-order rate constants and the half-life of AMX are presented for the reaction between gnZVI and AMX.

Ghauch et al. (2009) studied the degradation kinetics of AMX by traditional nZVI (produced with sodium borohydride) with an AMX/nZVI molar ratio of 1:8211, much higher than those used in this work. Under these conditions, a k_{obs} of $0.016 \pm 0.002 \text{ min}^{-1}$ was obtained with an amoxicillin half-life of $42.2 \pm 4.2 \text{ min}$.

Table 1 Observed first-order rate constants and the half-life of amoxicillin for the reaction of gnZVI with amoxicillin

Amoxicillin/gnZVI molar ratio	k_{obs} (min^{-1})	$t_{1/2}$ (min)	r^2
1:1.5	0.000171	4062	0.9923
1:7.5	0.000460	1507	0.9999
1:15	0.000880	788	0.9983
1:75	0.001247	556	0.9966

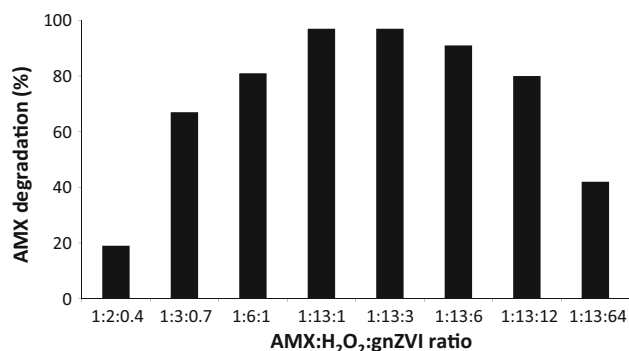


Fig. 4 Degradation of AMX in aqueous solutions by Fenton reaction catalyzed with gnZVI with different AMX:H₂O₂:Fe(II) ratios

Degradation of AMX through gnZVI-catalyzed Fenton reaction in aqueous solution

In order to evaluate the different applications of gnZVI for remediation processes, its use as a catalyst for the Fenton reaction was also tested. The use of nZVI with AMX was already performed but, to the best of the author's knowledge, no tests have ever been done with gnZVI.

Figure 4 shows the results obtained in the tests with different AMX/hydrogen peroxide/gnZVI molar ratios. After 15 min, the degradation efficiencies ranged from 19 to 97%, the highest being attained with 1:13:1 and 1:13:3 molar ratios. This indicates that the degradation is faster and more efficient than the degradation with gnZVI alone showing that the gnZVI can also be used for the degradation of AMX as a catalyst for the Fenton reaction, not only achieving high degradation efficiencies but also faster reactions (15 min).

According to Zha et al. (2014), the AMX is possibly adsorbed at the surface of the gnZVI where reacts with the OH radicals forming intermediate products, first to *m/z* 203(C₈H₁₂O₃NS), then to *m/z* 221 (C₈H₁₄O₄NS) by unfolding of the b-lactam ring and afterward to *m/z* 239

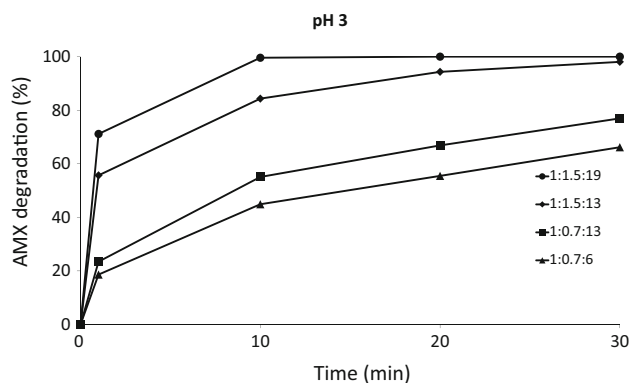


Fig. 5 Degradation of AMX in aqueous solutions by Fenton reaction at pH 3

(C₈H₁₆O₅NS) and the *m/z* 301(C₈H₁₄O₉NS). The reaction can proceed until CO₂ and H₂O are produced.

Comparing these results with those presented by Zha et al. (2014), who used nZVI produced by the traditional sodium borohydride method, it is clear that the application of gnZVI provided similar degradation efficiencies (around 80%) but with a much lower AMX/H₂O₂/ZVI ratio; 1:13:1 for gnZVI and 1:48:65 for nZVI, being both test were performed at pH 3. One of the advantages that the gnZVI have over the borohydride nZVI is the capacity of the natural extract that is in the gnZVI solution to enhance bioremediation, as shown in Fig. 3, meaning that the remaining amount of AMX could be eliminated through biological degradation when gnZVI is used.

In Table 2, the values of the observed first-order rate constants and the half-life of AMX are presented for the gnZVI-catalyzed Fenton reaction. The *k*_{obs} increases until an AMX/H₂O₂/gnZVI ratio of 1:13:3 and decreases for higher ratios. The *k*_{obs} obtained in the best test (1:13:1 ratio) is three times lower than the one presented by Zha et al. (2014), who used a much higher molar ratio. This proves that the use of gnZVI as a catalyst in the Fenton reaction could be an alternative to the traditional borohydride nZVI.

Table 2 Observed first-order rate constants and the half-life of the degradation of amoxicillin using the Fenton reaction catalyzed with gnZVI

Amoxicillin/H ₂ O ₂ /gnZVI molar ratio	<i>k</i> _{obs} (min ⁻¹)	<i>t</i> _{1/2} (min)	<i>r</i> ²
1:3:0.7	0.00925	74.9	0.9335
1:6:1	0.02628	26.4	0.9918
1:13:1	0.04996	13.9	0.9966
1:13:3	0.07778	8.9	0.9485
1:13:6	0.03351	20.7	0.9501
1:13:12	0.03122	22.2	0.9997

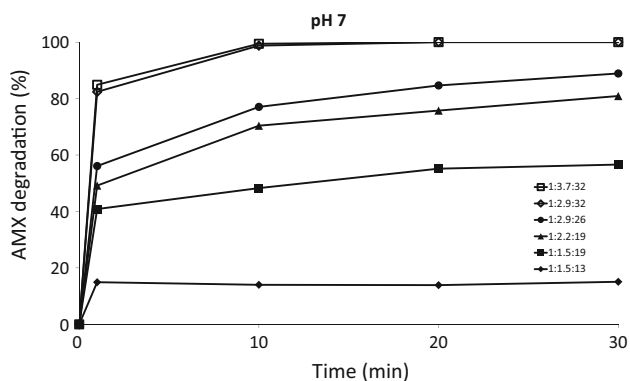


Fig. 6 Degradation of AMX in aqueous solutions by Fenton reaction at pH 7

Considering the results of Tables 1 and 2, it can be concluded that when the gnZVI are used as a catalyst for the Fenton reaction, the k_{obs} are significantly higher (>60 times) and the AMX half-life is much lower than those obtained when the gnZVI are used as reducing agent.

Finally, degradation tests were performed using the traditional Fenton reaction at pH 3 and 7 (Figs. 5, 6, respectively). Comparing these results Fig. 5 with those obtained with the gnZVI-catalyzed Fenton reaction (Fig. 4), it can be concluded that the gnZVI tests needed similar reagent ratios (1:13:3 for the gnZVI-catalyzed Fenton reaction and 1:19:1.5 for the traditional Fenton reaction) to achieve similar degradation efficiencies. This shows that the gnZVI-catalyzed Fenton reaction could become a greener alternative to the traditional Fenton reaction for the degradation of AMX.

Considering the influence of the pH of the solution on the degradation process, it is clear that at a lower pH the degradation efficiencies are higher (as expected for the Fenton reaction) due to the iron chemistry, namely iron hydroxides and oxides formation. Tests performed with the same molar ratio (1:13:1) used in the gnZVI-catalyzed process resulted in degradation efficiencies of 94% at pH 3 and 14% at pH 7 after 20 min. Although it is possible to reach 100% degradation of AMX at pH 7, much higher molar ratios would be needed.

Remediation of a sandy soil

After the tests performed with aqueous solutions, similar tests were performed with a sandy soil (pH from 2.6 to 3.4), spiked with AMX (5 mg kg^{-1}). As in the aqueous tests, gnZVI was tested as reductant and as a catalyst for the Fenton reaction. To the best of our knowledge, this is the

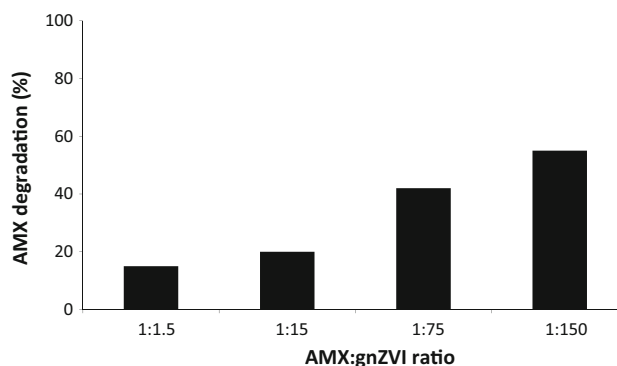


Fig. 7 Degradation of AMX in a sandy soil by gnZVI

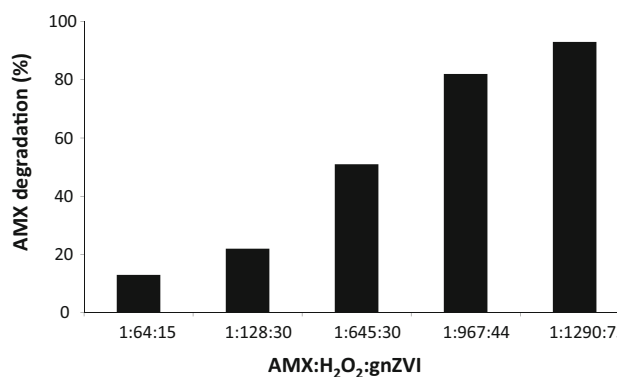


Fig. 8 Degradation of AMX in a sandy soil by solutions by Fenton reaction catalyzed with gnZVI with different AMX/H₂O₂/Fe(II) molar ratios

first work in which the chemical remediation of soils containing AMX is demonstrated.

Reduction of AMX in soil by gnZVI

Figure 7 shows the results obtained in the remediation tests of sandy soils spiked with AMX using gnZVI as reductant, with different AMX/gnZVI molar ratios (from 1:1.5 to 1:150), and after a reaction time of 360 min. Comparing the results of Fig. 7 with those in Fig. 1, it can be stated that the remediation tests performed in sandy soils had much lower degradation efficiencies. This could be due to parallel reactions of the gnZVI with the soil matrix, with the oxygen in the soil porosity, limitations on the dispersion of the nanoparticles in the soil, leading to situations where some parts of the soil were not reached by the gnZVI, and/or nanoparticle agglomeration that could lead to reduced mobility (Mystrioti et al. 2015).

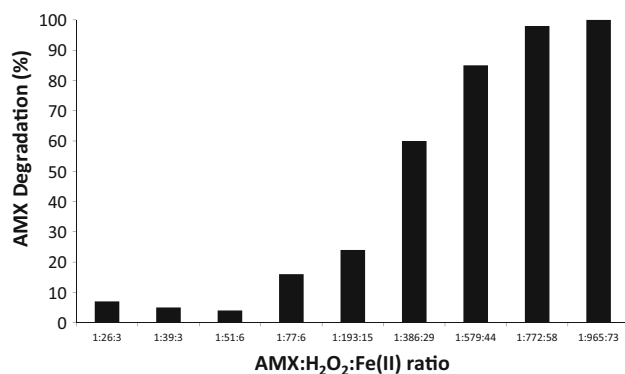


Fig. 9 Degradation of AMX in a sandy soil by Fenton reaction

As observed in the tests in aqueous media, more specifically what is illustrated in Fig. 2, the natural extracts are capable to enhance and promote biodegradation of AMX. This behavior was also observed in the soil tests where the degradation efficiencies reached 40, 53, 74 and 90% after 1800 h (data not shown) for the tests with molar ratios of 1:1.5, 1:15, 1:75 and 1:150, respectively. This confirms a great advantage of the use of gnZVI for AMX degradation.

Degradation of AMX in soil through a gnZVI-catalyzed Fenton reaction

Figure 8 shows the results obtained in the remediation tests of soils spiked with AMX using the gnZVI-catalyzed Fenton reaction, with different AMX/H₂O₂/gnZVI molar ratios.

The results show that it is possible to degrade up to 100% of AMX in the soil, although requiring extremely high AMX/H₂O₂/gnZVI molar ratios. This means that high quantities of reagents (the molar ratios are more than 100 times higher than those used in the aqueous tests) are required to achieve the remediation goals, therefore, increasing the remediation costs. The reasons pointed out above for the increase in the reagent requirements also explain these results. A similar discussion is applicable to the results in Fig. 9 that illustrate the results obtained in the degradation of AMX in a sandy soil by the traditional Fenton reaction.

By comparing the results of Figs. 8 and 9, it can be concluded that the Fenton reaction and the gnZVI-catalyzed Fenton reaction provide similar results; however, the former requires less quantities of hydrogen peroxide. Nevertheless, both tests proved that for soil remediation,

the reagent requirements are much higher than those for the remediation of aqueous solutions.

Conclusion

This work showed that green zero-valent iron nanoparticles (gnZVIs) are able to degrade up to 100% of AMX in aqueous systems and in soils, representing a viable alternative to nZVI produced with sodium borohydride. For remediation purposes, the gnZVIs can be used either as a reductant or as a catalyst in a Fenton-like reaction.

In aqueous systems, a degradation efficiency near 100% was achieved after 95 min with a 1:15 AMX/gnZVI molar ratio. The use of gnZVI showed another important advantage: the capacity of the natural extracts to enhance the biodegradation of AMX. This effect was observed after 100–120 h. The use of gnZVI as a catalyst for the Fenton reaction for the degradation of AMX showed to be more attractive because it presented degradation efficiencies of 100% after only 15 min, when a molar ratio of 1:13:1 (AMX/H₂O₂/gnZVI) was used.

In the soil tests, when gnZVI was used as a reducing agent, a decrease in the degradation efficiencies (to $\pm 60\%$) was observed. This is probably because of parallel reactions of the gnZVI with the soil matrix, limitation of the distribution of the nanoparticles in the soil and/or nanoparticle agglomeration. However, AMX was completely degraded after 1800 h. The use of gnZVI as a catalyst for the Fenton reaction resulted in near total degradation of AMX, although extremely high AMX/H₂O₂/gnZVI molar ratios were needed to achieve this goal.

Acknowledgements This work received financial support from the European Union (FEDER funds through COMPETE) and National Funds (FCT, Fundação para a Ciência e a Tecnologia) through Projects UID/QUI/50006/2013 and PTDC/AAG-TEC/2692/2012.

References

- Blowes DW, Ptacek CJ, Benner SG, McRae CWT, Bennett TA, Puls RW (2000) Treatment of inorganic contaminants using permeable reactive barriers. *J Contam Hydrol* 45:123–137. doi:10.1016/S0169-7722(00)00122-4
- Chrysochoou M, Johnston CP, Dahal G (2012) A comparative evaluation of hexavalent chromium treatment in contaminated soil by calcium polysulfide and green-tea nanoscale zero-valent iron. *J Hazard Mater* 201–202:33–42
- Cundy AB, Hopkinson L, Whithy RLD (2008) Use of iron-based technologies in contaminated land and groundwater remediation:

- a review. *Sci Total Environ* 400:42–51. doi:10.1016/j.scitotenv.2008.07.002
- Ghauch A, Tuqan A, Assia HA (2009) Antibiotic removal from water: elimination of amoxicillin and ampicillin by microscale and nanoscale iron particles. *Environ Pollut* 157:1626–1635. doi:10.1016/j.envpol.2008.12.024
- Gottschalk F, Kost E, Nowack B (2013) Engineered nanomaterials in water and soils: a risk quantification based on probabilistic exposure and effect modeling. *Environ Toxicol Chem* 32:1278–1287. doi:10.1002/etc.2177
- Gupta VK, Kumar R, Nayak A, Saleh TA, Barakat MA (2013) Adsorptive removal of dyes from aqueous solution onto carbon nanotubes: a review. *Adv Colloid Interface Sci* 193–194:24–34. doi:10.1016/j.cis.2013.03.003
- Hoag GE, Collins JB, Holcomb JL, Hoag JR, Nadagouda MN, Varma RS (2009) Degradation of bromothymol blue by ‘greener’ nanoscale zero-valent iron synthesized using tea polyphenols. *J Mater Chem* 19:8671–8677. doi:10.1039/B909148C
- Karlsson MNA, Deppert K, Wacaser BA, Karlsson LS, Malm JO (2005) Size-controlled nanoparticles by thermal cracking of iron pentacarbonyl. *Appl Phys A* 80:1579–1583. doi:10.1007/s00339-004-2987-1
- Karn B, Kuiken T, Otto M (2009) Nanotechnology and in situ remediation: a review of the benefits and potential risks. *Environ Health Perspect* 117:1823–1831. doi:10.1289/ehp.0900793
- Kuang Y, Wang QP, Chen ZL, Megharaj M, Naidu R (2013) Heterogeneous Fenton-like oxidation of monochlorobenzene using green synthesis of iron nanoparticles. *J Colloid Interface Sci* 410:67–73. doi:10.1016/j.jcis.2013.08.020
- Kuhn LT, Bojesen A, Timmermann L, Nielsen MM, Mørup S (2002) Structural and magnetic properties of core–shell iron–iron oxide nanoparticles. *J Phys Condens Matter* 14:13551
- Li XQ, Elliott DW, Zhang WX (2006) Zero-valent iron nanoparticles for abatement of environmental pollutants: materials and engineering aspects. *Crit Rev Solid State Mater Sci* 31:111–122. doi:10.1080/10408430601057611
- Machado S, Pinto SL, Grosso JP, Nouws HPA, Albergaria JT, Delerue-Matos C (2013a) Green production of zero-valent iron nanoparticles using tree leaf extracts. *Sci Total Environ* 445–446:1–8. doi:10.1016/j.scitotenv.2012.12.033
- Machado S et al (2013b) Application of green zero-valent iron nanoparticles to the remediation of soils contaminated with ibuprofen. *Sci Total Environ* 461–462:323–329. doi:10.1016/j.scitotenv.2013.05.016
- Machado S, Grosso JP, Nouws HPA, Albergaria JT, Delerue-Matos C (2014) Utilization of food industry wastes for the production of zero-valent iron nanoparticles. *Sci Total Environ* 496:233–240. doi:10.1016/j.scitotenv.2014.07.058
- Machado S, Pacheco JG, Nouws HPA, Albergaria JT, Delerue-Matos C (2015) Characterization of green zero-valent iron nanoparticles produced with tree leaf extracts. *Sci Total Environ* 533:76–81. doi:10.1016/j.scitotenv.2015.06.091
- Matlochova A, Placha D, Rapantova N (2013) The application of nanoscale materials in groundwater remediation. *Pol J Environ Stud* 22:1401–1410
- Mystrioti C, Papassiopi N, Xenidis A, Dermatas D, Chrysochoou M (2015) Column study for the evaluation of the transport properties of polyphenol-coated nanoiron. *J Hazard Mater* 281:64–69. doi:10.1016/j.jhazmat.2014.05.050
- Nägele E, Moritz R (2005) Structure elucidation of degradation products of the antibiotic amoxicillin with ion trap MSN and accurate mass determination by ESI TOF. *J Am Soc Mass Spectrom* 16:1670–1676. doi:10.1016/j.jasms.2005.06.002
- O’Hannesin SF, Gillham RW (1998) Long-term performance of an in situ “iron wall” for remediation of VOCs. *Ground Water* 36:164–170. doi:10.1111/j.1745-6584.1998.tb01077.x
- Saleh TA, Gupta VK (2011) Functionalization of tungsten oxide into MWCNT and its application for sunlight-induced degradation of rhodamine B. *J Colloid Interface Sci* 362:337–344. doi:10.1016/j.jcis.2011.06.081
- Saleh TA, Gupta VK (2012) Column with CNT/magnesium oxide composite for lead(II) removal from water. *Environ Sci Pollut Res* 19:1224–1228. doi:10.1007/s11356-011-0670-6
- Saleh TA, Alhooshani KR, Abdelbassit MSA (2015) Evaluation of AC/ZnO composite for sorption of dichloromethane, trichloromethane and carbon tetrachloride: kinetics and isotherms. *J Taiwan Inst Chem Eng* 55:159–169. doi:10.1016/j.jtice.2015.04.004
- Saravanan R, Shannkar H, Rajasudha G, Stephen A, Natayanan V (2011) Photocatalytic degradation of organic dye using nano ZnO. *Int J Nanosci* 10:253–257. doi:10.1142/S0219581X11007867
- Saravanan R, Karthikeyan S, Gupta VK, Sekaran G, Narayanan V, Stephen A (2013) Enhanced photocatalytic activity of ZnO/CuO nanocomposite for the degradation of textile dye on visible light illumination. *Mater Sci Eng C* 33:91–98. doi:10.1016/j.msec.2012.08.011
- Stefaniuk M, Oleszczuk P, Ok YS (2016) Review on nano zerovalent iron (nZVI): from synthesis to environmental applications. *Chem Eng J* 287:618–632. doi:10.1016/j.cej.2015.11.046
- Tratnyek PG, Johnson RL (2006) Nanotechnologies for environmental cleanup. *Nano Today* 1:44–48. doi:10.1016/s1748-0132(06)70048-2
- Waalewijn-Kool PL, Ortiz MD, van Straalen NM, van Gestel CAM (2013) Sorption, dissolution and pH determine the long-term equilibration and toxicity of coated and uncoated ZnO nanoparticles in soil. *Environ Pollut* 178:59–64. doi:10.1016/j.envpol.2013.03.003
- Wang C-B, Zhang W-x (1997) Synthesizing nanoscale iron particles for rapid and complete dechlorination of TCE and PCBs. *Environ Sci Technol* 31:2154–2156. doi:10.1021/es970039c
- Wang W, Zhou MH, Mao QO, Yue JJ, Wang X (2010) Novel NaY zeolite-supported nanoscale zero-valent iron as an efficient heterogeneous Fenton catalyst. *Catal Commun* 11:937–941. doi:10.1016/j.catcom.2010.04.004
- Wang Y, Zhou DM, Wang YJ, Wang L, Cang L (2012) Automatic pH control system enhances the dechlorination of 2,4,4’-trichlorobiphenyl and extracted PCBs from contaminated soil by nanoscale Fe-0 and Pd/Fe-0. *Environ Sci Pollut Res* 19:448–457. doi:10.1007/s11356-011-0587-0
- Wang D, Yang P, Zhu Y (2014) Growth of Fe₃O₄ nanoparticles with tunable sizes and morphologies using organic amine. *Mater Res Bull* 49:514–520. doi:10.1016/j.materresbull.2013.09.019
- Xu LJ, Wang JL (2013) Degradation of 4-chloro-3,5-dimethylphenol by a heterogeneous fenton-like reaction using nanoscale zero-valent iron catalysts. *Environ Eng Sci* 30:294–301. doi:10.1089/ees.2012.0025
- Yan WL, Lien HL, Koel BE, Zhang WX (2013) Iron nanoparticles for environmental clean-up: recent developments and future outlook. *Environ Sci Process Impacts* 15:63–77. doi:10.1039/c2em30691c
- Zha SX, Cheng Y, Gao Y, Chen ZL, Megharaj M, Naidu R (2014) Nanoscale zero-valent iron as a catalyst for heterogeneous Fenton oxidation of amoxicillin. *Chem Eng J* 255:141–148. doi:10.1016/j.cej.2014.06.057